ACADEMIC PRESS

Available online at www.sciencedirect.com

SCIENCE DIRECT®

DEVELOPMENTAL BIOLOGY

Developmental Biology 257 (2003) 153–165

www.elsevier.com/locate/ydbio

Orphan nuclear receptor βFTZ-F1 is required for muscle-driven morphogenetic events at the prepupal–pupal transition in *Drosophila melanogaster*

Tina M. Fortier, Priya P. Vasa, and Craig T. Woodard*

Department of Biological Sciences, Mount Holyoke College, South Hadley, MA 01075, USA

Received for publication 5 November 2002, revised 24 December 2002, accepted 27 December 2002

Abstract

In *Drosophila melanogaster*, fluctuations in 20-hydroxyecdysone (ecdysone) titer coordinate gene expression, cell death, and morphogenesis during metamorphosis. Our previous studies have supported the hypothesis that βFTZ-F1 (an orphan nuclear receptor) provides specific genes with the competence to be induced by ecdysone at the appropriate time, thus directing key developmental events at the prepupal–pupal transition. We are examining the role of βFTZ-F1 in morphogenesis. We have made a detailed study of morphogenetic events during metamorphosis in control and *βFTZ-F1* mutant animals. We show that leg development in *βFTZ-F1* mutants proceeds normally until the prepupal–pupal transition, when final leg elongation is delayed by several hours and significantly reduced in the mutants. We also show that *βFTZ-F1* mutants fail to fully extend their wings and to shorten their bodies at the prepupal–pupal transition. We find that *βFTZ-F1* mutants are unable to properly perform the muscle contractions that drive these processes. Several defects can be rescued by subjecting the mutants to a drop in pressure during the normal time of the prepupal–pupal transition. Our findings indicate that βFTZ-F1 directs the muscle contraction events that drive the major morphogenetic processes during the prepupal–pupal transition in *Drosophila.*

Keywords: Ecdysone; Imaginal discs; Larval muscles; Metamorphosis; Morphogenesis

Introduction

The development of animal body structures requires precise coordination of many complex processes. This coordination is often achieved by hormonal signaling. For example, the construction of a leg in the fruit fly, *Drosophila melanogaster*, involves the orchestration of numerous morphogenetic events by the single steroid hormone, 20-hydroxyecdysone (referred to here as ecdysone). *Drosophila* leg development thus provides an ideal model system in which to examine the control of specific developmental processes by steroid hormones. In directing leg formation and other developmental processes that occur during *Drosophila* metamorphosis, ecdysone acts in cooperation with a number of factors, including the orphan nuclear receptor βFTZ-F1 (Broadus et al., 1999; Woodard et al., 1994). We are examining the role of βFTZ-F1 in directing leg development and other morphogenetic processes that occur in response to ecdysone during metamorphosis in *Drosophila.*

Imaginal discs are epithelial sacs that are formed during embryogenesis and give rise to parts of the adult epidermis and cuticle, including the wings and legs. During larval development, the cells of the imaginal discs multiply and acquire their proper fates and positions (Cohen, 1993). Formation of the mature adult leg begins at the end of larval stages, when a high-titer pulse of ecdysone triggers puparation (puparium formation), which marks the beginning of the prepupal period and the onset of metamorphosis. This late larval ecdysone pulse directs the process of leg disc evagination, which transports the leg from the inside to the outside of the body and includes two different morphological events: initial elongation and shaping of the appendage, and eversion of the appendage to the outside of the animal.

* Corresponding author. Fax: +1-413-538-2548.
E-mail address: cwoodard@mtholyoke.edu (C.T. Woodard).

0012-1606/03/$ – see front matter
doi:10.1016/S0012-1606(03)00036-8

During initial elongation, from approximately 6 h before pupariation until 6 h after puparium formation (APF), morphogenesis of the leg disc begins with the telescoping of the flat disc into a long tubular limb. Increase in length is partly accomplished by the unfolding of the epithelium and a selective change in cell shape (Fristrom and Fristrom, 1993). Prior to metamorphosis, cells in the dorsal–lateral regions of the leg discs are anisometric, meaning that they are compressed in the proximal–distal axis and are elongated circumferentially (Condic et al., 1991). During appendage elongation, these anisometric cells become isometric, with increased length along the proximal–distal axis, resulting in leg elongation. Ecdysone induces these changes in cell shape, which are thought to account for most of the elongation in the basitarsal and tibial leg segments between 0 and 6 h APF (Condic et al., 1991). These transformations in cell shape result from myosin-based shaping of the actin cytoskeleton and contraction of the cortical belt, in a response that involves the rho signaling pathway (Edwards and Kiehart, 1996; Halsell et al., 2000).

At approximately 10–12 h APF, the prepupal pulse of ecdysone occurs, inducing pupation, the transition from prepupa to pupa. According to Chadfield and Sparrow (1985), the first visible event in this prepupal–pupal transition is the expulsion of the gas bubble from inside the animal into the posterior end of the puparium, where a local separation of the pupal cuticle from the puparium occurs. The abdomen then contracts rhythmically, forcing the gas to the anterior of the puparium. The prepupa gradually moves posteriorly, making a space at the anterior end, beneath the operculum. Contraction of larval abdominal muscles is believed to then cause an increase in internal pressure, which drives head eversion, as well as the inflation and final elongation of the legs and wings (Chadfield and Sparrow, 1985; Handler, 1982). Leg development, involving both cell division and expansion of cells, continues in the subsequent pupal stage (Chadfield and Sparrow, 1985; Handler, 1982). The events of the pupal stage also include completion and apolysis of the pupal cuticle, the final shaping of the appendages, differentiation of hairs and sensory structures, and deposition of the adult cuticle.

Mutational analyses have implicated a number of genes in leg morphogenesis, including *βFTZ-F1* (Broadus et al., 1999), *Broad-Complex (BR-C)* (Kiss et al., 1988), *spaghetti-squash (sqh)* (Edwards and Kiehart, 1996), and *Stubble (Sb)* (Beaton et al., 1988). The leg imaginal discs of *Stubble* and *spaghetti-squash* mutants do not undergo proper cell shape changes and elongation during the first 6 h of metamorphosis, resulting in the malformed leg phenotype (mlf), which includes curved, thickened upper legs. The mlf leg possesses all required segments, but those segments that depend most heavily on cell shape change for their adult appearance (femur, tibia, and basitarsus) are affected in shape and size (von Kalm et al., 1995). Certain combinations of *BR-C* mutant alleles also result in severe mlf phenotypes (von Kalm et al., 1995).

βFTZ-F1 is one of two protein isoforms encoded by *FTZ-F1,* which maps to the 75CD mid-prepupal puff locus. βFTZ-F1 is expressed widely throughout the animal at the larval molts and briefly during the mid-prepupal period (Lavorgna et al., 1993; Woodard et al., 1994; Yamada et al., 2000). A growing body of evidence strongly suggests that βFTZ-F1 acts as a competence factor for ecdysone induction of early genes. Ectopic expression of βFTZ-F1 from a transgene enhances the ecdysone induction of the early genes *BR-C, E74A,* and *E75A* and enables the premature induction of *E93* by ecdysone in cultured third instar larval salivary glands (Woodard et al., 1994). A loss-of-function mutation in *βFTZ-F1* results in pupal lethality, with defects in the expression of *BR-C, E74A, E75A,* and *E93* transcripts in the late prepupal stage (Broadus et al., 1999). *βFTZ-F1* mutants also exhibit defects in destruction of the larval salivary glands by programmed cell death (Lee and Baehrecke, 2001; Lee et al., 2002) and defects in head eversion and leg elongation. These mutants possess legs that are properly segmented but shorter than normal (Broadus et al., 1999). *βFTZ-F1* mutant legs have a malformed appearance very similar to that seen in mutants such as *Sb, BR-C,* and *sqh.* If βFTZ-F1 plays a role in directing the cell shape changes that occur within the first 6 h APF, then *βFTZ-F1* mutants should show leg defects early in metamorphosis similar to those seen in *Sb, BR-C,* and *sqh* mutants. An alternative possibility is that βFTZ-F1 directs the muscular response to the prepupal ecdysone pulse, which drives head eversion, and leg and wing elongation at the end of the prepupal stage (Chadfield and Sparrow, 1985; Fristrom and Fristrom, 1993). If this is correct, then *βFTZ-F1* mutants should display defective muscular contractions at the prepupal–pupal transition. These two possibilities are not mutually exclusive, however, and βFTZ-F1 may function in both the early and the later processes.

Here, we describe experiments testing these two hypotheses. We demonstrate that the leg imaginal discs of *βFTZ-F1* loss-of-function mutants show no defects in cell shape changes and develop normally through the prepupal stage. We also show that *βFTZ-F1* mutants are unable to contract their abdominal muscles normally, and therefore cannot generate sufficient internal pressure at the prepupal–pupal transition to inflate and elongate their legs and wings and evert their heads. Our findings indicate that βFTZ-F1 directs muscle contractions that drive the major morphogenetic events at the prepupal–pupal transition.

Materials and methods

Drosophila stocks

FTZ-F1^{17} (or *βFTZ-F1*^{17}) is described in Broadus et al. (1999), and *FTZ-F1*^{19} was isolated in the same mutagenesis and screen. The *FTZ-F1*^{19} allele carries a deletion that breaks approximately 0.5 kb 5′ of the *βFTZ-F1* transcrip-

tion start site and removes transcribed sequences in the common region of *FTZ-F1* (data not presented). *FTZ-F1*^{19} is most likely a null allele with respect to *βFTZ-F1* function. Both *FTZ-F1*^{17} and *FTZ-F1*^{19} were maintained over *TM6B, Tb Hu e*. Canton-S (CS), and *w*^{1118}; *P{w*$^{+}$*mW.hs = GawB}Dll*^{md23}*/CyO*, were obtained from the Bloomington *Drosophila* Stock Center. *w*^{1118}; *P[UAS-GFP*^{1521}*w*$^{+}$*]*; *Df(3L)*^{CatDH104}*/TM6B, Tb Hu e* was a gift from Julie Broadus. *Df(3L)Cat*^{DH104}*/TM6B, Tb Hu e (DfCat/TM6B, Tb Hu e*) was provided by Kristin White. *red Sb*^{63b}*e/TM6B, Tb Hu e* was a gift from Laurence von Kalm.

Maintenance of Drosophila stocks

The animals were cultured in glass or plastic bottles and vials and provided with yeasted fly food containing cornmeal, yeast, malt, and agar. These stocks were maintained in an incubator at a constant temperature of 25°C. Unless otherwise indicated, all experiments were carried out at 25°C.

Phalloidin staining of leg imaginal discs for cell shape and disc length studies

Fluorescent phalloidin (Alexa Fluor 488 from Molecular Probes), an actin stain, was used to visualize leg imaginal disc cell outlines in studies that compared cell shape changes in 0-h and 6-h APF control and mutant prepupae. Zero-hour (white) prepupae were collected from control (*w*^{1118}, *+/DfCat* and *Sb*^{63}) and mutant (*FTZ-F1*^{17}*/DfCat* and *FTZ-F1*^{17}*/FTZ-F1*^{19}) stocks and dissected in oxygenated, sterile Robb's saline (Robb, 1969) at room temperature. Leg discs were then selected and fixed in 4% formaldehyde solution overnight (18–24 h) at 4°C. Following fixation, the discs were permeabilized for 1–2 h with 0.5% Triton X-100 (w/v in PBS) at room temperature, and stained with a 0.6 μM phalloidin solution for 4 h also at room temperature. The discs were then rinsed with 0.5% Triton X-100 (w/v in PBS) for 2 h, with five to six changes at room temperature, and mounted in Vectashield (Vector Laboratories) for viewing with a BioRad MRC 600 laser scanning confocal microscope (Nikon inverted Diaphot base). The excitation wavelength required to view the green fluorescent phalloidin was set at 495 nm. The discs were examined by using confocal microscopy, with particular attention paid to the shape of cells in the proximal segments of the leg disc.

In order to perform cell shape studies on control and mutant 6-h prepupal leg discs, 0-h prepupae were selected and maintained at 25°C for a period of 6 h before dissection. The cell shapes observed in the proximal regions of the control and mutant 6-h APF leg discs were compared with each other, and with their corresponding regions in the 0-h discs. The length of control and mutant 6-h APF leg discs was also measured, and the average lengths were compared statistically. Control leg discs were obtained from CS wild-type, *w*^{1118}, and *+/DfCat* animals, while mutant leg discs were dissected from *FTZ-F1*^{17}*/DfCat* animals. A two-tailed *t* test was used to note any significant differences in leg disc length between each of the controls and the mutant. Unless otherwise indicated, uncertainties are expressed as standard deviation.

Visualizing leg development in living animals

In order to follow the progression of leg development in living prepupae and pupae, we generated animals expressing high levels of green fluorescent protein (GFP) specifically in the leg imaginal discs and developing legs. Due to faint GFP expression in the wings, we were also able to observe the later phases of wing elongation in this manner. The control genotype was constructed by crossing *w*^{1118}; *P[UAS-GFP*^{1521}*w*$^{+}$*]* virgin females with *w*^{1118}; *P{w*$^{+}$*mW.hs = GawB}Dll*^{md23}*/CyO* males. The *βFTZ-F1* mutant genotype was made by crossing *w*^{1118}; *P{w*$^{+}$*mW.hs = GawB}Dll*^{md23}*/P[UAS-GFP*^{1521}*w*$^{+}$*]*; *DfCat/TM6B, Tb Hu e* virgin females with *w*^{1118}; *P{w*$^{+}$*mW.hs = GawB}Dll*^{md23}*/P[UAS-GFP*^{1521}*w*$^{+}$*]*; *FTZ-F1*^{17}*/TM6B, Tb Hu e* males. Leg morphogenesis was visualized by using a modified protocol developed in the Thummel lab (Ward et al., 2003). Animals of the appropriate genotype were collected as 0-h prepupae and placed in a moist chamber made from a modified culture dish. The animals were viewed with a BioRad MRC 600 laser scanning confocal microscope (Nikon inverted Diaphot base) for a period of up to 51.5 h at a constant temperature of 19°C. Images were captured at 6-min intervals, and these data were converted into time-lapse movies. The corresponding time for each image from the movie (see Figs. 3 and 4) is represented as (hr:min) APF. For example, 0 h APF is (00:00). A QuickTime movie is available at http://www.mtholyoke.edu/courses/cwoodard/legmovies/fly.html.

Observations of control and βFTZ-F1 mutant whole animals during pupation

To further characterize pupation, time-lapse video recordings were made of control and mutant development. Animals were collected at 0 h APF and placed in a modified moist chamber. A video recording system consisting of an Olympus SZH Stereo Microscope, Sony DXC-970MD 3CCD Color Video Camera, SONY CMA-D2 Camera Adaptor, Panasonic Time-Lapse Video Cassette Recorder 6740, and SONY Trinitron Monitor was used to make time-lapse (18 h) video recordings starting at 0 h APF and ending at 18–24 h APF. Recordings were analyzed noting the developmental timeline and the quality and duration of specific movements. The length to which legs extended toward the posterior end of the animal was measured by determining the denticle belt (on the pupal case) reached by the tips of the most posterior pair of legs. Denticle belt #10

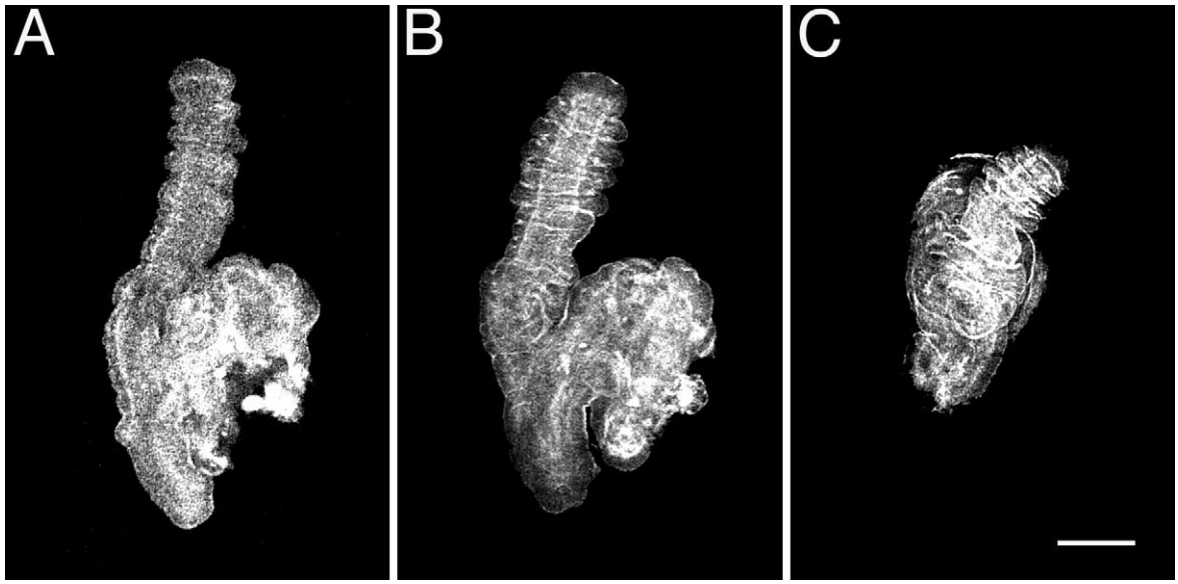

Fig. 1. Low magnification confocal images of control (w^{1118}) and *βFTZ-F1* mutant (*FTZ-F1*^{17}/*FTZ-F1*^{19}) 6-h prepupal leg discs. Leg discs from 6-h prepupae were dissected, fixed, stained with fluorescent phalloidin, and viewed. Leg disc length was measured by using a calibrated micrometer (see Materials and methods). (A) Control. (B) *FTZ-F1* mutant. At this stage, similar shape and length of both sets of leg discs can be observed. (C) A leg disc from a *Stubble* mutant, *Sb*^{63b}, in which defective cell shape changes result in malformed, short legs is included for comparison. Calibration bar is 130 μm.

is most posterior, and belt #1 is most anterior. In cases where legs extended to a point halfway between two belts, the extension was recorded to the nearest half denticle belt. For example, extension of the leg tips to a point halfway between denticle belts #5 and #6 was recorded as "5.5." Extension of the leg tips to a point halfway between denticle belt #10 and the extreme posterior end of the pupal case was recorded as "10.5." Length of wing extension was determined in the same way.

Comparing length of control and βFTZ-F1 mutant animals at 0, 14, and 19 h APF

To measure the length of prepupae and pupae, control (+/*DfCat*) and mutant (*FTZ-F1*^{17}/*DfCat*) 0-h prepupae were collected and either viewed and measured immediately as 0-h prepupae, or maintained at 25°C for a period of either 14 or 19 h in a moist culture dish chamber and then viewed. Animals were viewed on a compound microscope, and the lengths of their pupal cases were measured by using a calibrated micrometer. The length of the prepupa or pupa was then measured as viewed through the puparium. A statistical analysis of the average length of the control and mutant animals, with and without their pupal cases, was performed by using a two-tailed *t* test.

Rescue of FTZ-F1 mutants by a drop in pressure

To subject *FTZ-F1* mutant and control animals to a drop in pressure, a special apparatus was built. This device consisted of a vacuum pump connected through a water manometer to a sealed glass chamber. An animal of the appropriate genotype (Control or Mutant), aged 9.5 h APF, was placed in the glass chamber and attached to the floor of the chamber by using double-sided tape. The chamber was connected to the device and the pressure inside it was drawn down to a mean of 23 mmHg below ambient for a period of up to 10 h. Animals treated in this manner are referred to as "Treated." The animal was observed through a dissecting microscope, and the times of final leg and wing elongation and head eversion were recorded. The length to which legs and wings extended toward the posterior end of the animal was measured by determining the denticle belt reached by their most posterior points as described above. For each genotype, an additional group of animals, "Untreated," was kept at ambient pressure and observed in the same way as the Treated animals. Thus, there were four groups of animals in this analysis—"Control Treated," "Control Untreated," "Mutant Treated," and "Mutant Untreated." A statistical analysis of the average length of the legs in each group was performed by using a two-sample *t* test. Length of wing extension was determined in the same way.

Fig. 2. High magnification confocal images of the (A) control (calibration bar is 30 μm) and (B) *βFTZ-F1* mutant 6-h prepupal leg discs show the successful transformation from anisometric (compressed in the proximal–distal axis and elongated circumferentially) cells to isometric (with increased length along the proximal–distal axis) cells in the basitarsal and tibial segments. (C) A similar image of a leg disc from a *Sb*^{63b} mutant, in which this transformation has failed, is shown for comparison. Arrows point to cells in the basitarsal and tibial segments. Calibration bar for (B) and (C) is 20 μm.

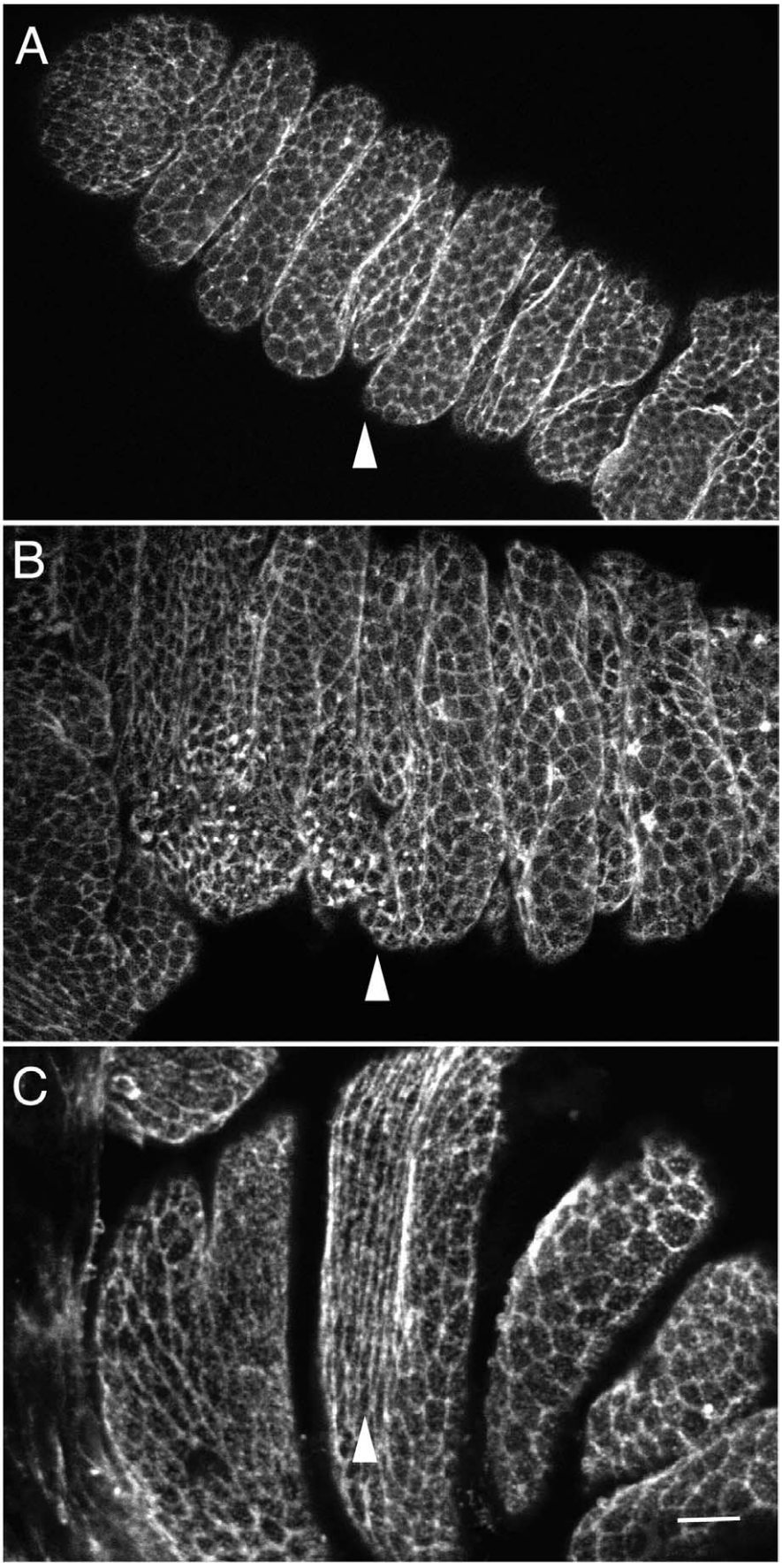
A
B
C

Results

Cell shape changes occur normally between 0 and 6 h APF in βFTZ-F1 mutant leg imaginal discs

βFTZ-F1 is expressed widely throughout the animal in the very late embryo and at the larval molts before its appearance during the mid-prepupal stage (Lavorgna et al., 1993; Yamada et al., 2000). To confirm that the defects in adult leg morphology of our *βFTZ-F1* mutants do not occur before the mid-prepupal expression of *βFTZ-F1*, phalloidin-stained 0-h prepupal leg imaginal discs of mutant animals were compared with those from control animals for similar morphology and size. The shape and size of leg imaginal discs from controls and *βFTZ-F1* mutants appear similar at this stage. Higher magnification confocal images showed characteristic anisometric (compressed in the proximal–distal axis) cells in the basitarsal and tibial regions of control (w^{1118}, and +/*DfCat*) and *βFTZ-F1* mutant (*FTZ-F1*^{17}*/DfCat*, and *FTZ-F1*^{17}*/FTZ-F1*^{19}) 0-h prepupal leg discs (data not presented).

We investigated the possibility that defective cell shape changes in early prepupal leg imaginal discs account for the abnormally short, but correctly segmented legs seen in *βFTZ-F1* mutants. Leg imaginal discs from control and *βFTZ-F1* mutant 6-h prepupae were dissected and stained with phalloidin, then visualized by using confocal microscopy. Fig. 1 shows low magnification confocal images of control and *βFTZ-F1* mutant 6-h APF prepupal leg discs. Control and *βFTZ-F1* mutant leg discs showed similar shape and length. A leg disc from a *Stubble* mutant, Sb^{63b}, in which defective cell shape changes result in malformed, short legs, is included for comparison. Two-sample *t* test analysis of average leg disc length at 6 h APF revealed no significant differences ($P = 0.47$) between those of *FTZ-F1* mutants (0.94 ± 0.12 mm, $n = 27$) and controls (0.87 ± 0.19 mm, $n = 5$).

Higher magnification confocal images of the control and βFTZ-F1 mutant leg discs show the successful transformation of cells from anisometric to isometric in the basitarsal and tibial segments (Fig. 2). A high magnification image of leg discs from an Sb^{63b} mutant, in which this transformation has failed, is shown for comparison. These findings indicate that wild-type levels of βFTZ-F1 are not required for the very early events of leg morphogenesis.

βFTZ-F1 mutants fail to extend their legs fully at the prepupal–pupal transition

In order to determine exactly when the defect in leg development occurs in the *βFTZ-F1* mutants, we examined leg development through the first 51.5 h of metamorphosis in living animals. Leg development in older prepupae and pupae takes place inside the darkened puparium, making visualization difficult. To solve this problem, we constructed control genotype and *βFTZ-F1* mutant animals expressing GFP in the developing leg imaginal discs and legs, as described (Ward et al., 2003). These animals also express low levels of GFP in their wings, enabling us to observe some aspects of wing development. This technique, along with our very careful observations using light microscopy, has allowed us to examine the morphogenetic events of *Drosophila* metamorphosis at a level of detail that was previously not possible. A QuickTime movie is available at http://www.mtholyoke.edu/courses/cwoodard/legmovies/fly.html. Figs. 3 and 4 show still images from this movie, in which a control animal and a *βFTZ-F1* mutant animal (see Materials and methods), both expressing GFP in the leg imaginal discs, were collected together as 0-h prepupae, and imaged side-by-side for a period of 51.5 h by using a confocal microscope. In both the control and the mutant animals, the second pair of legs (T2 legs) are elongated and visible at 0 h APF (00:00 in Fig. 3). The first (T1) pair of legs, obscured by the T2 legs, is visible between 2 and 3 h APF, and the third (T3) pair of legs, between 4 and 5 h APF. The process of leg eversion begins at 5 h APF and is completed by the time the wings appear, which is by 06:00 (Fig. 3). The period of leg elongation that follows occurs in two phases. The first phase is completed by about 7 h APF, and is followed by a second, lesser phase of elongation at about 9 h APF. By 10 h APF, the legs and wings have temporarily ceased to elongate, and they remain at this length until the final elongation event, which occurs during the prepupal–pupal transition.

As expected, there is no detectable difference between the *βFTZ-F1* mutant and control until just before head eversion, when a dramatic anterior translocation of the legs occurs. The control animal begins this translocation process at about 12:00, and its legs reach the most anterior point by 13:36 (Fig. 3). At this point, the legs are aligned with the eye–antennal imaginal discs. Around 13:54, the final elongation event begins, and the legs and wings reach their final length by about 16:00 (Fig. 3).

Fig. 3. Defects in leg development seen in *βFTZ-F1* mutants at the prepupal–pupal transition. Still images from a time-lapse movie in which a control (top) and a *βFTZ-F1* mutant (bottom), both expressing GFP in the leg imaginal discs (and to a lesser degree in the wings), were collected together as 0-h prepupae, and imaged side-by-side for a period of 51.5 h by using a confocal microscope. Images were collected from the ventral side at 6-min intervals and compiled into a time-lapse movie, which can be viewed at http://www.mtholyoke.edu/courses/cwoodard/legmovies/fly.html. Corresponding times are shown in the upper right corner in hr:min APF. Arrows mark the onset of anterior leg translocation by 12 h APF (12:00), and the most anterior point reached by the legs at 13:36. The major elongation event begins by 13:54, and the developing legs and wings reach their final length by 16:00. Calibration bar is 500 μm.

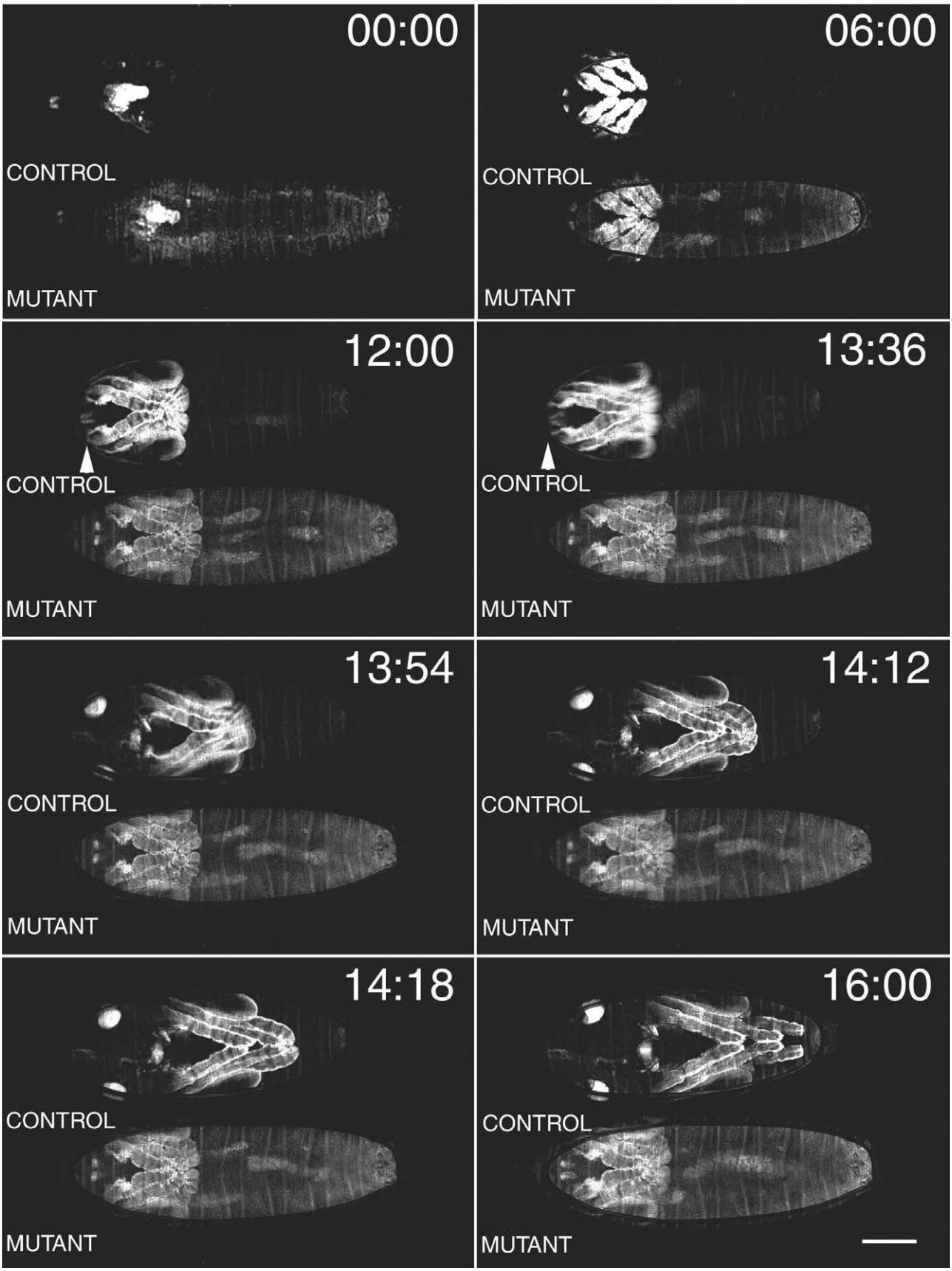
00:00
CONTROL
MUTANT
06:00
CONTROL
MUTANT
12:00
CONTROL
MUTANT
13:36
CONTROL
MUTANT
13:54
CONTROL
MUTANT
14:12
CONTROL
MUTANT
14:18
CONTROL
MUTANT
16:00
CONTROL
MUTANT

The legs of the *βFTZ-F1* mutant animal make a slight anterior shift at 17:00, reaching a most anterior position at 17:12 (Fig. 4). Unlike in the control animal, the mutant legs are never drawn far enough toward the anterior to align with the eye–antennal imaginal discs. Final leg and wing elongation begins by 17:18 and is complete by 17:30 (Fig. 4). Throughout the final elongation process, the mutant legs remain bent and never straighten as in the control animal. We observe more bending in the mutant up to about 18 h APF. Refinement is delayed in the mutant, beginning around 21:00 in the mutant (Fig. 4) as opposed to around 19 h APF in the control, but appears to proceed normally. All subsequent leg development in the mutant appears to occur normally at the proper time. At 50:00, the mutant legs appear normally segmented, but are short, thick, and bent (Fig. 4).

βFTZ-F1 mutants are defective in muscle-driven movements during the prepupal–pupal transition

We have employed a stereo microscope–time-lapse video recording system to capture the events that take place from 0 to 18 h APF, noting in particular the movements associated with the hallmark events leading up to and including final leg elongation. In control animals, pupation occurs as described (Chadfield and Sparrow, 1985; Robertson, 1936). *βFTZ-F1* mutants develop normally through most of the prepupal stage. Before 2 h APF, internal movements, including fluctuations, shifts up and down, short pulse-like, and wave-like contractions, are seen in the mid-abdominal cavity, corresponding to the area between denticle belts #6 and #8 of the pupal case. Between 2 and 4 h APF, the gas bubble is formed in this region. Pulses and wave-like contractions around the gas bubble start in a discrete region and eventually surround the entire bubble, translocating it toward the posterior end of the animal. The contractions become more vigorous as the process continues, and the gas bubble becomes less visible as the posterior tip of the abdomen retracts. Initial differences between the control and *βFTZ-F1* mutant animals can be seen during gas bubble translocation. In the control, the gas bubble reaches the extreme posterior end at approximately 12 h APF, when it is expelled from the animal into the space between the pupal cuticle and the puparium. In the mutant, translocation of the gas bubble to the posterior of the puparium is incomplete. A transluscent area persists in the mid-abdominal region occupied by the gas bubble, indicating the presence of residual gas, which is not seen in controls. This residual gas is often present until much later, when the mouthparts have been detached.

The *βFTZ-F1* mutant also shows defects in posterior retraction of the prepupal body and anterior gas movement. Posterior retraction begins later in the mutant (approximately 16–18 h APF) than in controls (approximately 12 h APF). In the mutant, retraction of the posterior tip of the abdomen is not a fluid process as it is in controls. This process occurs sporadically in the mutant, eventually bringing the posterior tip of the abdomen to between denticle belts #8 and #9, but never past denticle belt #8. In comparison, the control animal retracts from the posterior as far as denticle belt #7. As posterior retraction continues, the process of anterior gas movement begins. In the control, over the next 10–15 min, retractions, extensions, and lateral shifting movements of the posterior tip of the abdomen move the gas to the anterior region of the puparium. As the gas moves along the side of the animal toward the anterior, surface tension is broken, and ripples are formed between the pupal cuticle and the puparium. This rippling extends well into the thoracic region of the control, but in the mutant it never extends beyond denticle belt #5 or #6. The mutant appears immobilized in the mid to anterior thoracic region, whereas in the control, the animal swings freely back and forth in this area. Gas movement into the anterior occurs more quickly and efficiently in the control than in the mutant. This process, which creates space into which the head can evert, takes approximately 1 h in the mutant (compared with about 10 min in the control).

In the control, between 12 and 13 h APF, the anterior region of the body moves rhythmically side-to-side as the animal makes its way back into the posterior end of the puparium. This posterior translocation appears to be driven by rhythmic contractions of abdominal muscles. These side-to-side movements detach the mouthparts and allow the head to evert fully. The movements that detach the mouthhooks are less vigorous in the mutant and can take up to 20 min (as compared with 2 min in the control). The mutant never fully moves back into the posterior of the puparium, and the thoracic region still appears immobilized at 18 h APF.

The movements that detach the mouthhooks also drive the inflation of the legs and wings, which elongate incrementally, extending a bit further each time the muscles contract. By 15–16 h APF in the control, the legs and wings are fully extended, with the legs reaching approximately denticle belt #9, and the wings approximately denticle belt #7. In the *βFTZ-F1* mutant, these movements appear insufficient to fully inflate the legs and wings, which typically do not extend past denticle belt #6.

βFTZ-F1 mutants fail to shorten their bodies during metamorphosis

To further investigate the functionality of the larval abdominal musculature, we compared the lengths of control and *βFTZ-F1* mutant animals at 0, 14, and 19 h APF. The abdominal muscle contractions that elongate appendages and evert the head are also thought to cause the withdrawal of the prepupa from the puparium (pupal case), shortening it at pupation (Chadfield and Sparrow, 1985). The degree of body shortening was thus taken as an indication of contractile functionality. To make sure that the muscles were contracting normally at pupariation in the mutant, length mea-

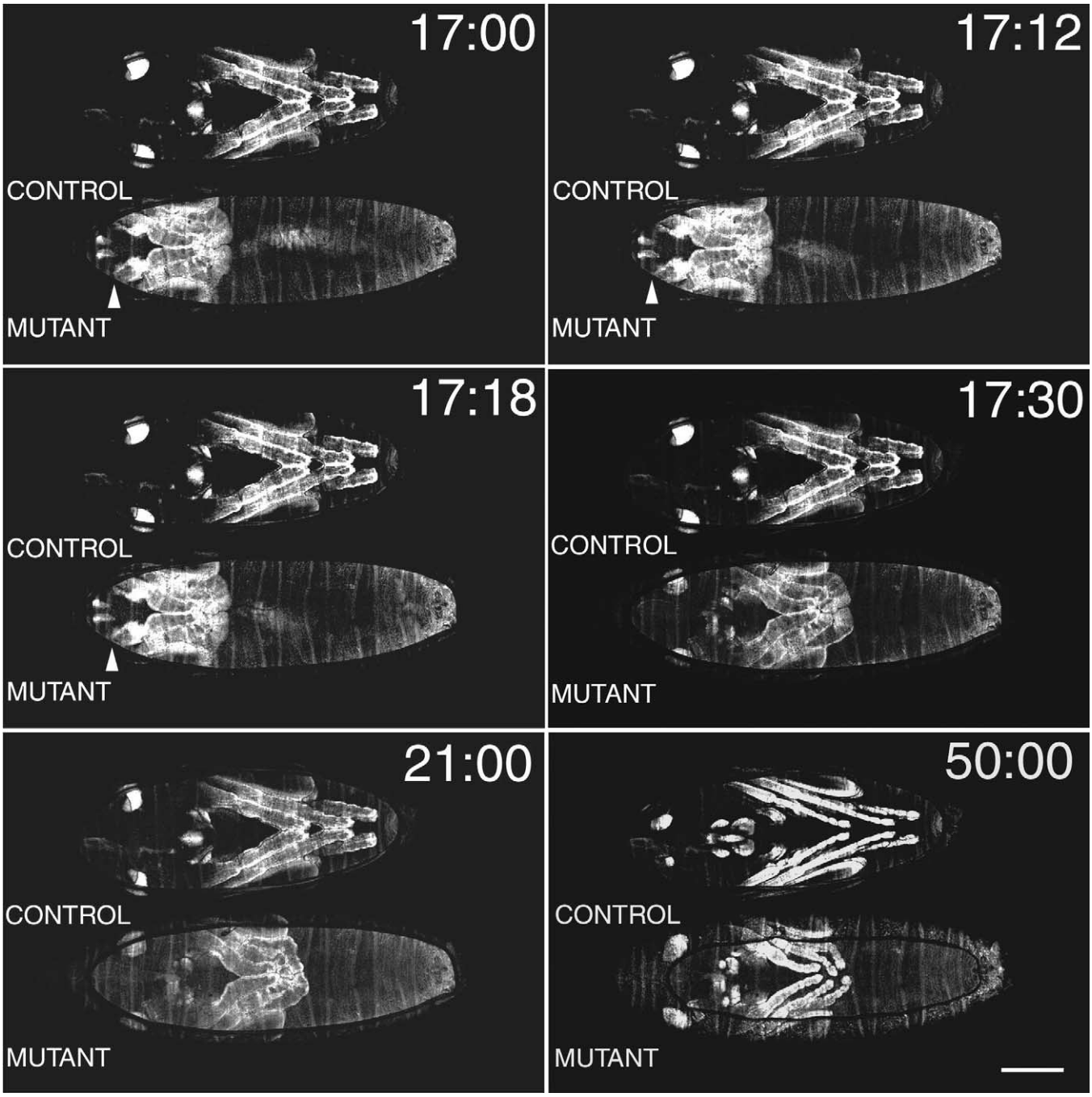

Fig. 4. *βFTZ-F1* mutants exhibit greatly reduced anterior leg translocation and final leg length. Representative images from the same time-lapse movie shown in Fig. 3. Control (top) and a *βFTZ-F1* mutant (bottom). Corresponding times are shown in the upper right corner in hr:min APF. Images were collected from the ventral side at 6-min intervals and compiled into a time-lapse movie, which can be viewed at http://www.mtholyoke.edu/courses/cwoodard/legmovies/fly.html. Arrows mark the onset of anterior leg translocation in the mutant by 17:00, and the most anterior point reached by the legs by 17:12. The final elongation event begins by 17:18, and final leg and wing length is reached by 17:30. Refinement of the legs begins at about 21:00 in the mutant [as opposed to about 19:00 (not shown here) in the control]. By 50:00, the mutant legs appear normally segmented but bent, and are shorter and thicker than control legs. Calibration bar is 500 μm.

surements were first conducted on control and *βFTZ-F1* mutant 0-h prepupae. The lengths of the prepupal body and the puparium were measured by using a calibrated micrometer. Table 1 shows the results of these studies. A two-tailed *t* test analysis of the average lengths of the control and mutant animals' bodies showed no significant difference at 0 h APF ($P = 0.82$). The length of their pupal cases also did not differ significantly at this stage ($P = 0.83$).

Length measurements were then made on animals following the prepupal–pupal transition, at 14 h APF and 19 h

Table 1
Length of control and *βFTZ-F1* mutants at 0 h, 14 h, and 19 h APF

Aged animals	*N*	Mean length[a] of prepupa or pupa (mm)	Control vs. mutant Sig. (2-tailed *t* test)	*N*	Mean length[a] of puparium (mm)	Control vs. mutant Sig. (2-tailed *t* test)
Control 0 h APF	11	1.02 ± 0.02	0.82	11	1.31 ± 0.07	0.83
Mutant 0 h APF	09	1.02 ± 0.02		09	1.32 ± 0.05	
Control 14 h APF	16	0.91 ± 0.05	0.0013	17	1.29 ± 0.07	0.15
Mutant 14 h APF	16	0.98 ± 0.04		22	1.32 ± 0.04	
Control 19 h APF	11	0.94 ± 0.05	0.0002	11	1.30 ± 0.07	0.17
Mutant 19 h APF	21	1.02 ± 0.04		21	1.33 ± 0.05	

[a] Mean length ± standard deviation.

APF. A two-tailed *t* test analysis of the average length of the control and mutant animal's bodies showed a significant difference at 14 h APF ($P = 0.0013$) and at 19 h APF ($P = 0.0002$). The length of the pupal case, however, was not affected in the mutant and did not differ significantly either at 14 h APF ($P = 0.15$) or 19 h APF ($P = 0.17$).

Defects in βFTZ-F1 mutants can be rescued by a drop in pressure

The muscular contractions believed to drive leg extension, as well as head eversion and wing extension, are thought to do so by causing an increase in the internal pressure of the animal. The inflation and extension of the legs and wings is thought to require the generation of greater pressure inside the developing legs than outside (Chadfield and Sparrow, 1985; Fristrom and Fristrom, 1993). We therefore hypothesized that *βFTZ-F1* mutants are defective in these muscle contractions and cannot generate sufficient internal pressure at the prepupal–pupal transition to drive these key developmental events. If this hypothesis is true, it should be possible to rescue *βFTZ-F1* mutants by exposing them to decreased external pressure, making their internal pressure effectively higher. Fristrom (1965) was able to drive head eversion prematurely in wild-type animals and in *cryptocephal* mutants by putting them in a chamber and exposing them to a drop in pressure. We attempted rescuing leg extension, wing extension, and head eversion in *βFTZ-F1* mutants by subjecting them to a decrease in pressure during the time when the prepupal–pupal transition and these events normally occur. In each experiment, an animal of the appropriate genotype, aged 9.5 h APF was subjected to a reduction in pressure averaging 23 mmHg below ambient for a period of up to 10 h. Table 2 shows that chamber treatment had no significant effect on leg length in control genotype animals ($P = 0.819$), but the reduced pressure resulted in a significant increase in leg length of *βFTZ-F1* mutant animals ($P = 0.002$).

The reduced pressure also had a rescue effect on wing length in the *βFTZ-F1* mutants (Table 2). The chamber treatment had no significant effect on wing length in control genotype animals ($P = 0.441$). In contrast, the reduced pressure resulted in a significant increase in wing length of *βFTZ-F1* mutant animals ($P = 0.002$).

The degree of rescue in the mutant from the reduced pressure treatment varied (Fig. 5). In most cases, the pressure drop resulted in only partial rescue of leg and wing extension, but 23.4% of the treated mutant animals were rescued to completion with regard to leg length (legs extend

Table 2
Rescue of leg and wing elongation in *βFTZ-F1* mutants by a drop in pressure

	N	Mean length[a]	Std. deviation	Std. error of the mean	Untreated vs. treated Sig. (2-tailed *t* test)
Legs					
Control Untreated	41	8.89	0.44	0.007	0.819
Control Treated	28	9.00	0.65	0.123	
Mutant Untreated	27	5.31	0.74	0.144	0.002
Mutant Treated	32	6.37	1.65	0.292	
Wings					
Control Untreated	41	7.74	0.43	0.007	0.441
Control Treated	28	7.76	0.42	0.008	
Mutant Untreated	27	5.17	0.44	0.008	0.002
Mutant Treated	32	5.97	1.26	0.223	

Note. "Untreated" animals were observed at ambient atmospheric temperature.
"Treated" animals were subjected to reduced pressure, as described in Materials and methods.
[a] The length to which legs or wings extended toward the posterior end of the animal was measured by determining the denticle belt (on the pupal case) reached by their most posterior tips. For further explanation of how leg and wing length were recorded, see Materials and methods.

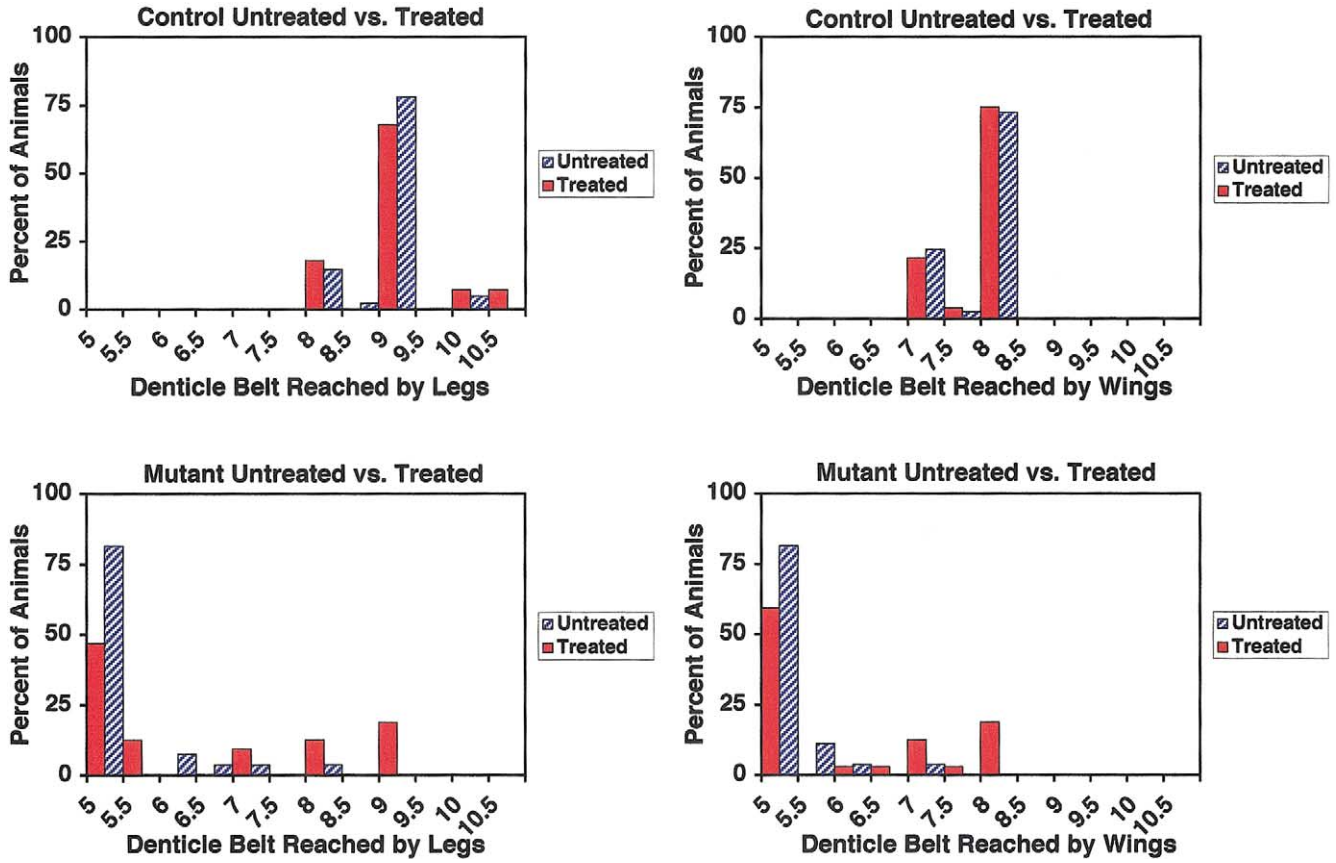

Fig. 5. Effects of reduced external pressure on final leg and wing length in control and *βFTZ-F1* mutants. An animal of the appropriate genotype (Control or *βFTZ-F1* Mutant), aged 9.5 h APF, was placed in the glass chamber and adhered to the floor of the chamber by using double-sided tape. The chamber was attached to the device, and the pressure inside it was drawn down to a mean of 23 mmHg below ambient for a period of up to 10 h. Animals treated in this manner are referred to as "Treated." The length to which legs and wings extended toward the posterior end of the animal was measured by determining the denticle belt reached by their most posterior points as described in Materials and methods. For each genotype, an additional group of animals, "Untreated," was kept at ambient pressure and observed in the same way as the Treated animals.

at least to denticle belt #8). Interestingly, in every case in which leg elongation was rescued to completion in the mutant, head eversion, wing extension, and gas bubble translocation were also rescued completely. None of the "completely rescued" mutant animals survived to eclosion, however.

Discussion

Wild-type βFTZ-F1 function is not required for the early events of leg disc elongation

Our findings here indicate that wild-type *βFTZ-F1* function is not required for morphogenetic processes that occur during the late larval and early prepupal stages. At 0 h APF, *βFTZ-F1* mutant leg discs appear normal, suggesting that βFTZ-F1 has no role in leg disc development prior to the beginning of metamorphosis. Leg discs examined at 6 h APF also showed no defects in length or in the cell shape changes required for the first phase of elongation, indicating that βFTZ-F1 is not involved in these early metamorphic events. The *βFTZ-F1* allele used in this study, $FTZ\text{-}F1^{17}$, is hypomorphic and is expressed at very low levels (Broadus et al., 1999). It is possible that these cell shape changes require only a minute amount of βFTZ-F1 and would not occur normally in the complete absence of this protein. Although this is a formal possibility, the evidence indicates that it is unlikely given the developmental expression pattern of *βFTZ-F1*. *βFTZ-F1* is expressed during the last larval molt (approximately 48 h before puparium formation), but is not expressed again until the mid-prepupal stage, beginning at about 5 h APF (Andres et al., 1993; Lavorgna et al., 1993; Yamada et al., 2000).

βFTZ-F1 is required for muscle contractions that drive the prepupal–pupal transition

βFTZ-F1 mutant legs develop normally until the prepupal–pupal transition. In the mutant, the anterior translocation and subsequent extension of the legs are delayed by several hours and are incomplete. All subsequent leg devel-

opment in the mutant appears to occur normally, indicating that the abnormalities seen in these mutants are in fact due to stage-specific defects, rather than to general weakness or ill-health.

In wild-type animals, during the prepupal–pupal transition, contractions of larval muscles shorten the prepupal body, translocate the mid-abdominal gas bubble to the posterior end of the pupal case, and then move the gas to the anterior, providing a space into which the head can evert (Robertson, 1936). These contractions have long been thought to generate hydrostatic pressure, inflating and elongating the legs and wings in the animal. Detailed observation of the *βFTZ-F1* mutants in this study revealed defects in each of these developmental processes. Furthermore, we have observed that, in *βFTZ-F1* mutants, the muscle contractions that drive these events are much less deliberate, vigorous, and consistent than in controls.

We show that gas bubble translocation, leg and wing elongation, and head eversion can be rescued by exposing mutant prepupae to decreased external pressure. This indicates that these defects result from failure to generate sufficient internal pressure at the appropriate time. This also provides direct evidence that hydrostatic pressure does in fact drive the major extensions of legs and wings at the prepupal–pupal transition. The observation that a drop in pressure can completely rescue leg elongation in some *βFTZ-F1* mutants suggests that there are no defects in the leg imaginal discs of these animals and indicates that βFTZ-F1 is required for the muscle contractions that drive major morphogenetic events at the prepupal–pupal transition. To test the possibility that abnormalities in muscle morphology account for these contractile defects, we have done both light microscopy and transmission electron microscopy (TEM) studies comparing musculature of control and *βFTZ-F1* mutant animals up to 12 h APF. We have detected no muscle differences between control and mutant animals (data not presented).

The increase in hydrostatic pressure that inflates and elongates the wings and legs during pupation normally occurs when the surrounding pupal cuticle is still incomplete (Fristrom and Fristrom, 1993; Handler, 1982). During wild-type metamorphosis, the development of the pupal cuticle is completed shortly after the prepupal–pupal transition. Therefore, in *βFTZ-F1* mutants, it is possible that the delay in muscle contraction results in this transition taking place within a rigid pupal cuticle, which does not allow complete head eversion, or extension of wings and legs. Another possibility is that abnormal cuticle formation or deposition may affect some events at pupation. The expression of *EDG78E* and *EDG84A*, genes that encode pupal cuticle proteins (Fechtel et al., 1988), is reduced and delayed in *βFTZ-F1* mutants (Broadus et al., 1999; Murata et al., 1996). If these proteins are not expressed properly, the cuticle may be abnormally rigid at the end of the prepupal stage. Thus, a greater force of contraction would be required to elongate the legs and wings to their normal length during the prepupal–pupal transition. Defective cuticle does not explain failed gas bubble translocation, however, so it appears that, in the *βFTZ-F1* mutant, muscle contractions are insufficient. Nonetheless, the notion of increased cuticular rigidity is an interesting concept that merits future exploration.

Our findings indicate that the major morphogenetic defects seen in *βFTZ-F1* mutants result from ineffective muscular contractions at the normal time of the prepupal–pupal transition. βFTZ-F1 regulates the expression of several genes during the late-prepupal stage, including *BR-C*, *E74A*, *E75A*, and *E93* (Broadus et al., 1999). The defects seen during pupation in the *βFTZ-F1* mutant are possibly due to the reduced expression of one or more of these, or other, target genes. We will attempt to determine which βFTZ-F1 target genes direct these morphogenetic events. Yamada et al. (2000) state that βFTZ-F1 is ubiquitously expressed in mid-prepupae. Further characterization of this expression pattern will be helpful in understanding the function of βFTZ-F1 in morphogenesis. As a competence factor that enables genes to respond to ecdysone at the right time in the proper cells, βFTZ-F1 has a pivotal position in directing the transformation from larva to adult. Elucidating the role of βFTZ-F1 in *Drosophila* metamorphosis will be an important step toward understanding how steroid hormones coordinate the complex events of animal development.

Acknowledgments

We thank Julie Broadus and Kristin White for *Drosophila* stocks. We thank George Cobb, Rachel Fink, Janice Gifford, Tamra Hjermstad, and Diane Kelly for technical assistance. We thank Sarah Bacon, Eric Baehrecke, and Carl Thummel for comments on the manuscript. We especially thank Pamela Reid for teaching us how to make the GFP movies. This work is supported by a National Science Foundation CAREER Award (MCB-9722205) and a National Science Foundation RUI Grant (MCB-0110238) (to C.T.W.).

References

Andres, A.J., Fletcher, J.C., Karim, F.D., Thummel, C.S., 1993. Molecular analysis of the initiation of insect metamorphosis: a comparative study of *Drosophila* ecdysteroid-regulated transcription. Dev. Biol. 160, 388–404.

Beaton, A.H., Kiss, I., Fristrom, D., Fristrom, J.W., 1988. Interaction of the *Stubble-stubbloid* locus and the *Broad-Complex* of *Drosophila melanogaster*. Genetics 120, 757–767.

Broadus, J., McCabe, J.R., Endrizzi, B., Thummel, C.S., Woodard, C.T., 1999. The *Drosophila* βFTZ-F1 orphan nuclear receptor provides competence for stage-specific responses to the steroid hormone ecdysone. Mol. Cell 3, 143–149.

Chadfield, C.G., Sparrow, J.C., 1985. Pupation in *Drosophila melanogaster* and the effect of the lethal *cryptocephal* mutation. Dev. Genet. 5, 103–114.

Cohen, S.M., 1993. Imaginal disc development, in: Arias, A.M. (Ed.), The Development of *Drosophila melanogaster*, Cold Spring Harbor Laboratory Press, Cold Spring Harbor, NY, pp. 747–841.

Condic, M.L., Fristrom, D., Fristrom, J.W., 1991. Apical cell shape changes during *Drosophila* imaginal disc elongation: a novel morphogenetic mechanism. Development 111, 23–33.

Edwards, K.A., Kiehart, D., 1996. *Drosophila* nonmuscle myosin II has multiple essential roles in imaginal disc and egg chamber morphogenesis. Development 122, 1499–1511.

Fechtel, K., Natzle, J.E., Brown, E.E., Fristrom, J.W., 1988. Prepupal differentiation of *Drosophila* imaginal discs: identification of four genes whose transcripts accumulate in response to a pulse of 20-hydroxyecdysone. Genetics 120, 465–474.

Fristrom, D., Fristrom, J.W., 1993. The metamorphic development of the adult epidermis, in: Martinez Arias, A. (Ed.), The Development of *Drosophila melanogaster*, II, Cold Spring Harbor Laboratory Press, Cold Spring Harbor, NY, pp. 843–897.

Fristrom, J.W., 1965. Development of the morphological mutant *cryptochephal* of *Drosophila melanogaster*. Genetics 52, 297–318.

Halsell, S.R., Chu, B.I., Kiehart, D.P., 2000. Genetic analysis demonstrates a direct link between Rho signaling and nonmuscle myosin function during *Drosophila* morphogenesis. Genetics 156, 1253–1265.

Handler, A.M., 1982. Ecdysteroid titres during pupal and adult development in *Drosophila melanogaster*. Dev. Biol. 93, 73–82.

Kiss, I., Beaton, A.H., Tardiff, J., Fristrom, D., Fristrom, J.W., 1988. Interactions and developmental effects of mutations in the *Broad-Complex* of *Drosophila melanogaster*. Genetics 118, 247–259.

Lavorgna, G., Karim, F.D., Thummel, C.S., Wu, C., 1993. Potential role for a FTZ-F1 steroid receptor superfamily member in the control of *Drosophila* metamorphosis. Proc. Natl. Acad. Sci USA 90, 3004–3008.

Lee, C., Baehrecke, E.H., 2001. Steroid regulation of autophagic programmed cell death during development. Development 128, 1443–1455.

Lee, C., Simon, C.R., Woodard, C.T., Baehrecke, E.H., 2002. Genetic mechanism for the stage- and tissue-specific regulation of steroid triggered programmed cell death in *Drosophila*. Dev. Biol. 252, 138–148.

Murata, T., Kageyama, Y., Hirose, S., Ueda, H., 1996. Regulation of the *EDG84A* gene by FTZ-F1 during metamorphosis in *Drosophila melanogaster*. Mol. Cell. Biol. 16, 6509–6515.

Robb, J.A., 1969. Maintenance of imaginal discs of *Drosophila melanogaster* in chemically defined media. J. Cell Biol. 41, 876–885.

Robertson, C.W., 1936. The metamorphosis of *Drosophila melanogaster*, including an accurately timed account of the principle morphological changes. J. Morphol. 59, 351–399.

von Kalm, L., Fristrom, D., Fristrom, J., 1995. The making of a fly leg: a model for epithelial morphogenesis. BioEssays 17, 693–702.

Ward, R.E., Reid, P., Bashirullah, A., D'Avino, P.P., Thummel, C.S., 2003. GFP in living animals reveals dynamic developmental responses to ecdysone during *Drosophila* metamorphosis. Dev. Biol., in press.

Woodard, C.T., Baehrecke, E.H., Thummel, C.S., 1994. A molecular mechanism for the stage-specificity of the *Drosophila* prepupal genetic response to ecdysone. Cell 79, 607–618.

Yamada, M., Murata, T., Hirose, S., Lavorgna, G., Suzuki, E., Ueda, H., 2000. Temporally-restricted expression of transcription factor *βFTZ-F1*: significance for embryogenesis, molting and metamorphosis in *Drosophila melanogaster*. Development 127, 5083–5092.